Chapter 4

Miscible Langmuir monolayers : Interactions between the polar head groups of cholesteryl acetate and octylcyanobiphenyl

4.1 Introduction

In the previous chapter we have presented the role played by the polar groups resulting in immiscible monolayer in Ch-8CB mixed system. In this chapter, we discuss the interactions between a weakly polar ester group of cholesteryl acetate(ChA) with strongly polar CN of 8CB. The hydrophobic core in ChA is the same as that in Ch whereas the hydrophilic head groups are different. Thus it helps to specifically investigate the role played by the weakly polar group of ChA. The hydrogen bonding tendency of the polar head group tends to inhibit the true equilibrium situation. Hence, a weakly polar group like ester with reduced hydrogen bonding ability is often chosen [1]. To stabilize a monolayer of a material with weakly polar group having important functional properties, it is mixed with a strongly polar molecule. This helps in transferring these films onto substrate with better transfer ratio and homogeneity. The nature of collapse pressure behavior and the condensation in A/M will reveal the nature of interactions in the mixed monolayer [2, 3].

4.2 Experiment

The experimental setup is identical to that discussed in chapter-3 for Ch-8CB mixed monolayer system. The structure of cholesteryl acetate is shown in Figure 4.1. In ChA, the ester polar group is less polar when compared with OH polar group of cholesterol. More importantly, it has relatively less hydrogen bonding ability. The ester group of ChA acts only as hydrogen bond acceptor whereas the alcohol group of Ch acts as both hydrogen bond donor and acceptor. The hydrogen bonding donor-acceptor interactions and their directionality have been discussed in detail [4]. The structure of 8CB which possess CN as polar group

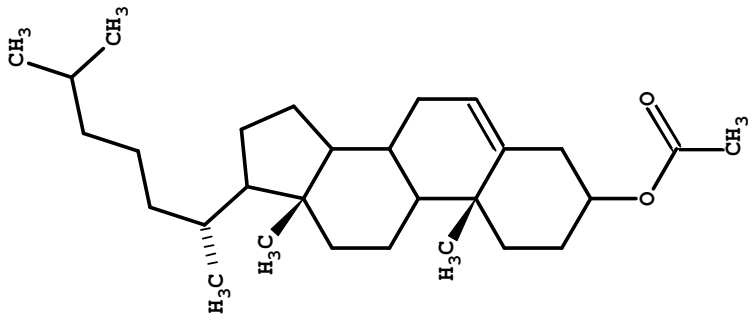

Figure 4.1: Structure of cholesteryl acetate(ChA)

is given in chapter-3(Figure 3.2). The surface manometry and epifluorescence techniques are mentioned in detail in chapter-3. Each isotherm at a particular mole fraction is repeated thrice and the difference in the A/M was less than ±0.3 $Å^2$. A moving point average of 20 points was used for these isotherms. This process had considerably brought down the noise level in the data which helped in deriving the compressional elastic modulus calculated from the π-A/M isotherm.

4.3 Results

The isotherm for the individual monolayers of ChA and 8CB are shown in Figure 4.2. The isotherm of ChA resembled that of Ch except for the decrease in the value of collapse pressure. The surface pressure is zero above 40 $Å^2$ and it increases rapidly and collapses at 15.4 mN/m. The limiting area per molecule, A_0, is 39.2 $Å^2$. After the collapse, there ex-

ists a plateau region which continues till 20Å^2 and at still lower A/M the surface pressure increases. The isotherm for 8CB is discussed in detail in chapter-3. The isotherm for the

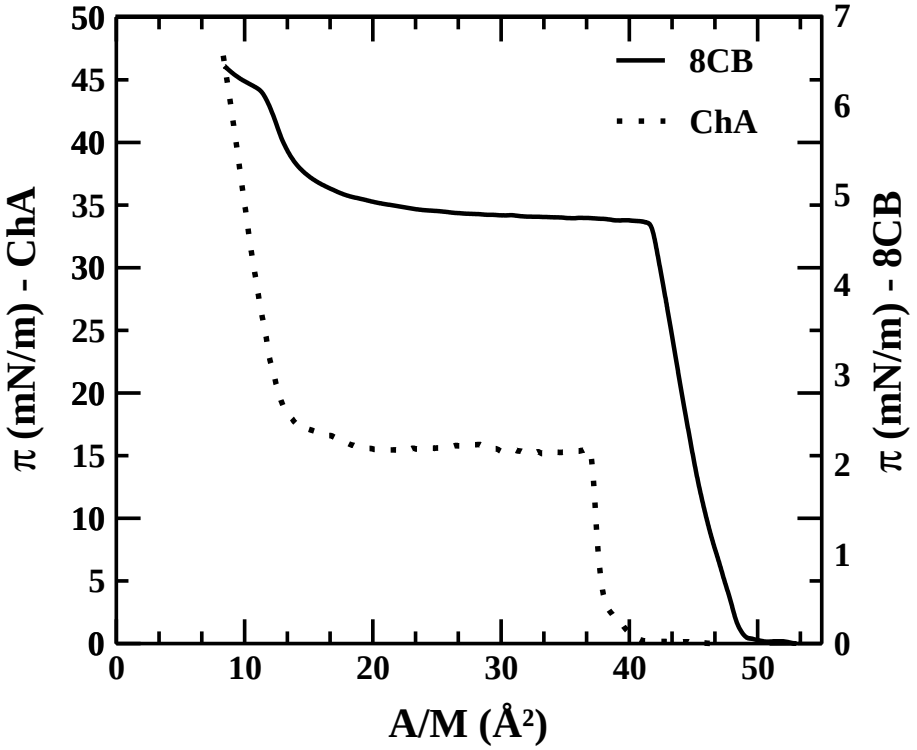

Figure 4.2: Surface pressure(π) - area per molecule(A/M) isotherm for cholesteryl acetate(ChA) and octylcyanobiphenyl(8CB) monolayer at t=22 °C. The vertical axis on the left gives the scale for ChA and the vertical axis on the right gives the scale for 8CB.

mixed monolayer of ChA and 8CB is shown in Figure 4.3. Interesting trend was observed in the collapse behavior for ChA-8CB mixed monolayer. The isotherms indicate the presence of two collapse pressures. The collapse behavior of the mixed monolayer will reveal the miscibility and stability. For an ideal case of *miscible* mixed monolayer, the collapse pressure of a monolayer A will vary continuously and will approach the collapse pressure of a monolayer B. For an immiscible mixed monolayer, the collapse pressures of individual molecules do not vary and will be independent of the composition. This implies that one will always observe two collapse pressures at all compositions. Figure 4.4 represents schematically the two cases. For the case of ChA-8CB mixed monolayer, the variation of collapse pressures with increasing mole fraction(MF) of ChA in 8CB is shown in Figure 4.5. Interestingly, a different type of collapse pressure behavior was observed for this system. The

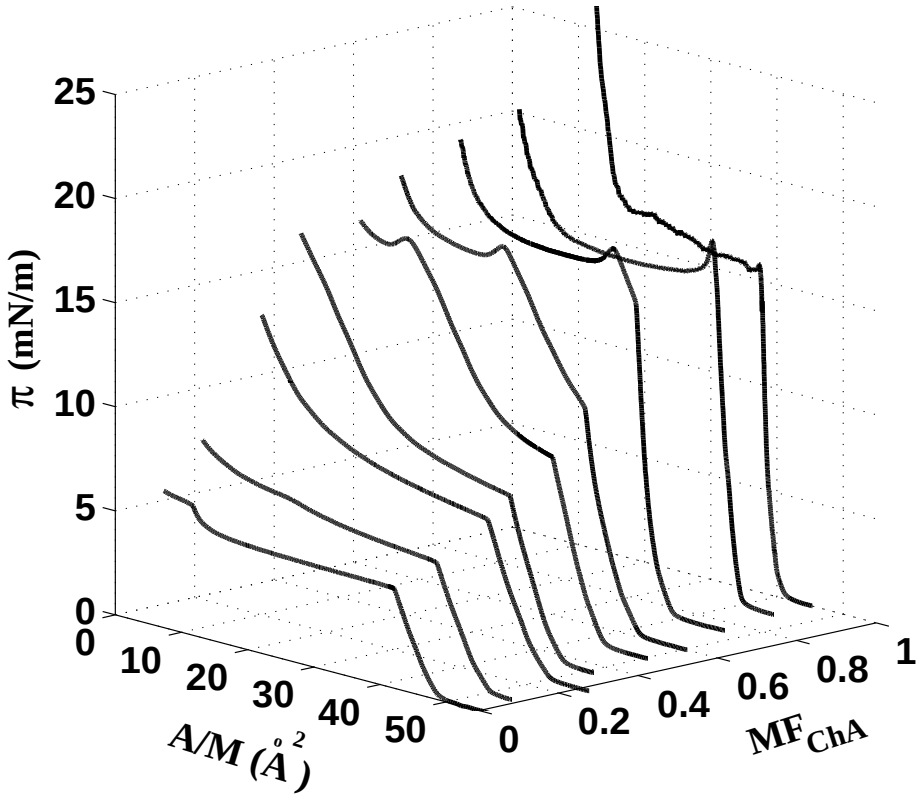

Figure 4.3: Surface pressure(π) - area per molecule(A/M) isotherms for ChA-8CB mixed monolayer at different mole fractions(MF) of ChA in 8CB at t=22 °C.

collapse pressure of lower magnitude, $\pi_{c(8CB)}$, varied continuously with composition of ChA. The higher collapse pressure, $\pi_{c(ChA)}$ was found to be independent of composition.

The compressional elastic modulus, $|E|$, of the mixed monolayer can be calculated from the isotherm using,

$$|E| = (A/M) * (d\pi/d(A/M)) \tag{4.1}$$

where A/M is the area per molecule and π is the surface pressure. The magnitude of compressional elastic modulus is different for different monolayer phases and it indicates the stability of the mixed monolayer [5]. In the case of ChA, the elastic modulus($|E|$) for ChA was 460.4 mN/m at a surface pressure of 10 mN/m. The variation of $|E|$ with π in the L_1 phase at different MF of ChA in ChA - 8CB mixed monolayer is shown in Figure 4.6. We find an increase in $|E|$ in the mixed monolayer with increasing MF of ChA.

The epifluorescence images for the individual 8CB and its phase sequences are de-

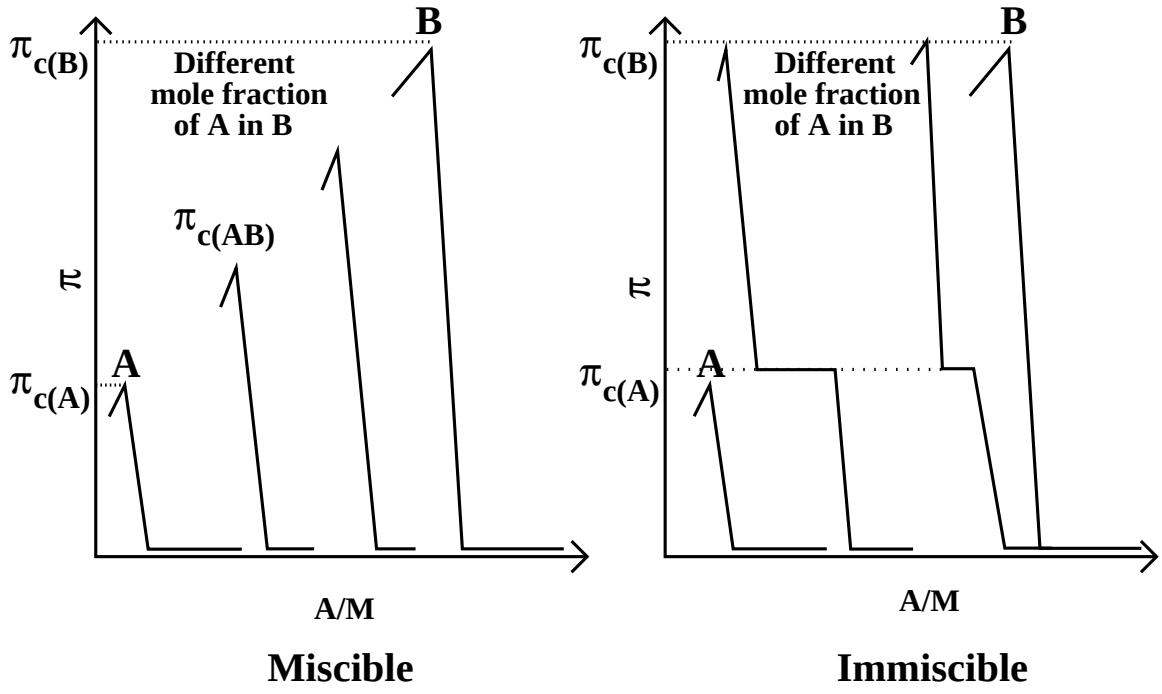

Figure 4.4: Nature of collapse pressure for ideal mixed monolayers of A and B. For miscible case, collapse pressure gradually increases for increasing mole fraction of A in B. For immiscible case, the two collapse pressures occur and it is independent of composition.

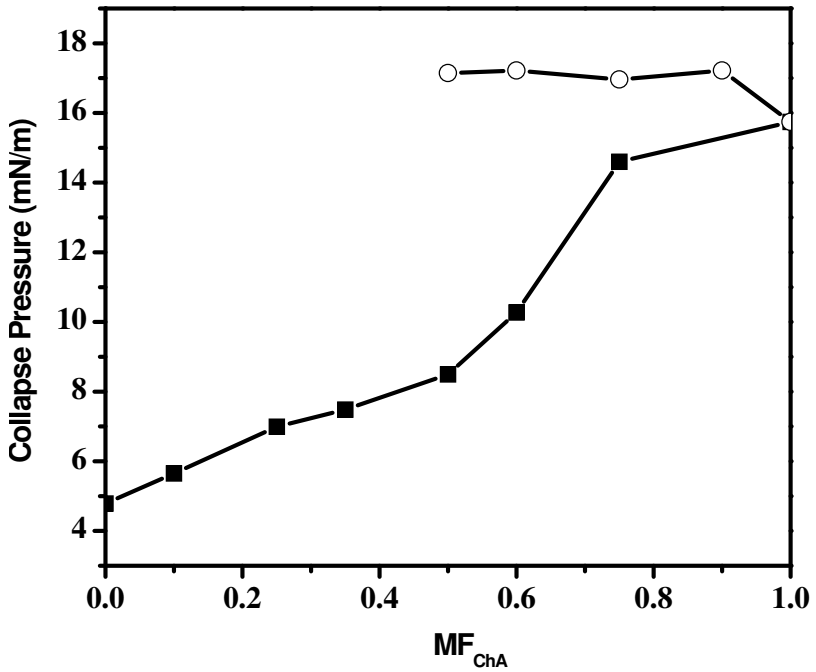

Figure 4.5: Variation of collapse pressure with mole fraction(MF) of ChA in 8CB. The filled square represent the lower collapse pressure, $\pi_{c(8CB)}$ and the open circles represent the higher collapse pressure, $\pi_{c(Ch)}$.

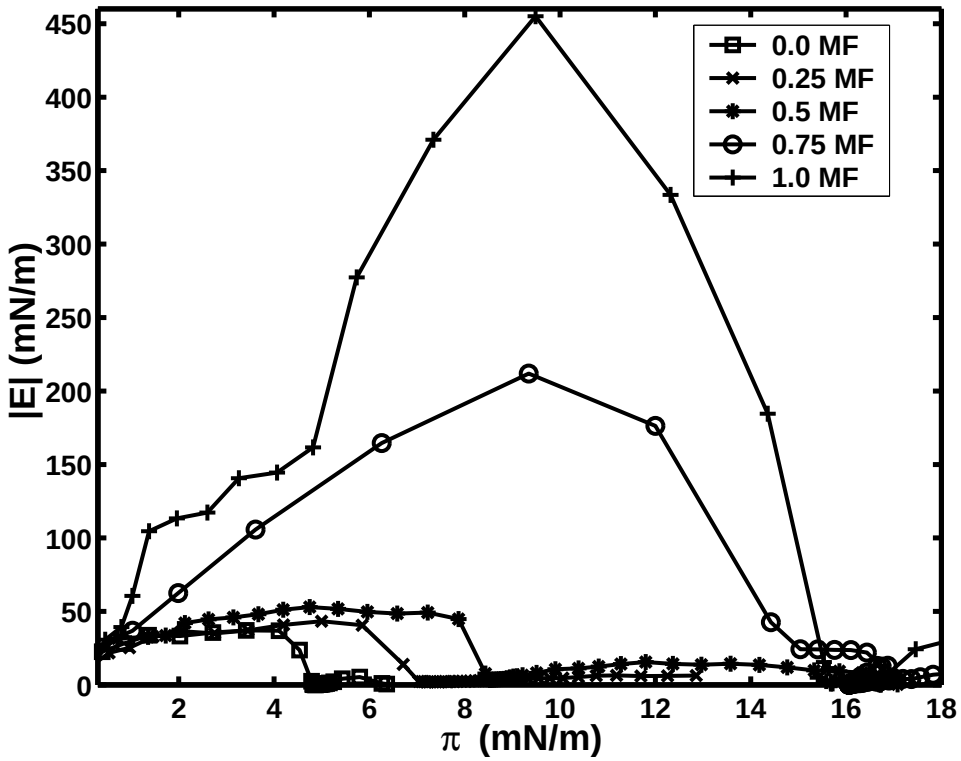

Figure 4.6: Variation of elastic modulus, $|E|$ with surface pressure, π at different mole fraction(MF) of ChA in 8CB.

scribed in the chapter-3. The epifluorescence images for ChA monolayer are shown in Figure 4.7. The textures of ChA are quite different from that of Ch. At very large A/M(> 130Å^2), the usual circular dark gas(G) domains coexist with bright L_2 domains in the background(Figure 4.7(a)). Figures 4.7(b) and 4.7(c) show the presence of L_2 phase which possess irregular boundaries. Upon compression, the circular gas domains diminishes in size. This is seen in Figures 4.7(d) and 4.7(e). The L_2 phase, occurs with bright and dark mesh texture(Figures 4.7(f) to 4.7(j)). After the collapse, dark elongated crystallites of ChA was found to nucleate from the L_2 phase(Figures 4.7(k) and 4.7(l)). The epifluorescence images for 0.25 MF of ChA in 8CB is shown in Figure 4.8. The mixed monolayer exhibits the usual gas(dark) + L_1 coexistence phase. The L_1 phase appeared homogeneous and was of uniform intensity. Above the lower collapse, 8CB squeezes resulting in multilayers(Figures 4.8(a) and 4.8(b)). Here, the transformation occurs from L_1 phase to D_2 multilayers occurs phase without the formation of three layer(D_1) phase. Upon compression, the number of D_2 domains and its intensity increases. This is shown in the Figures 4.8(c) to 4.8(f). The

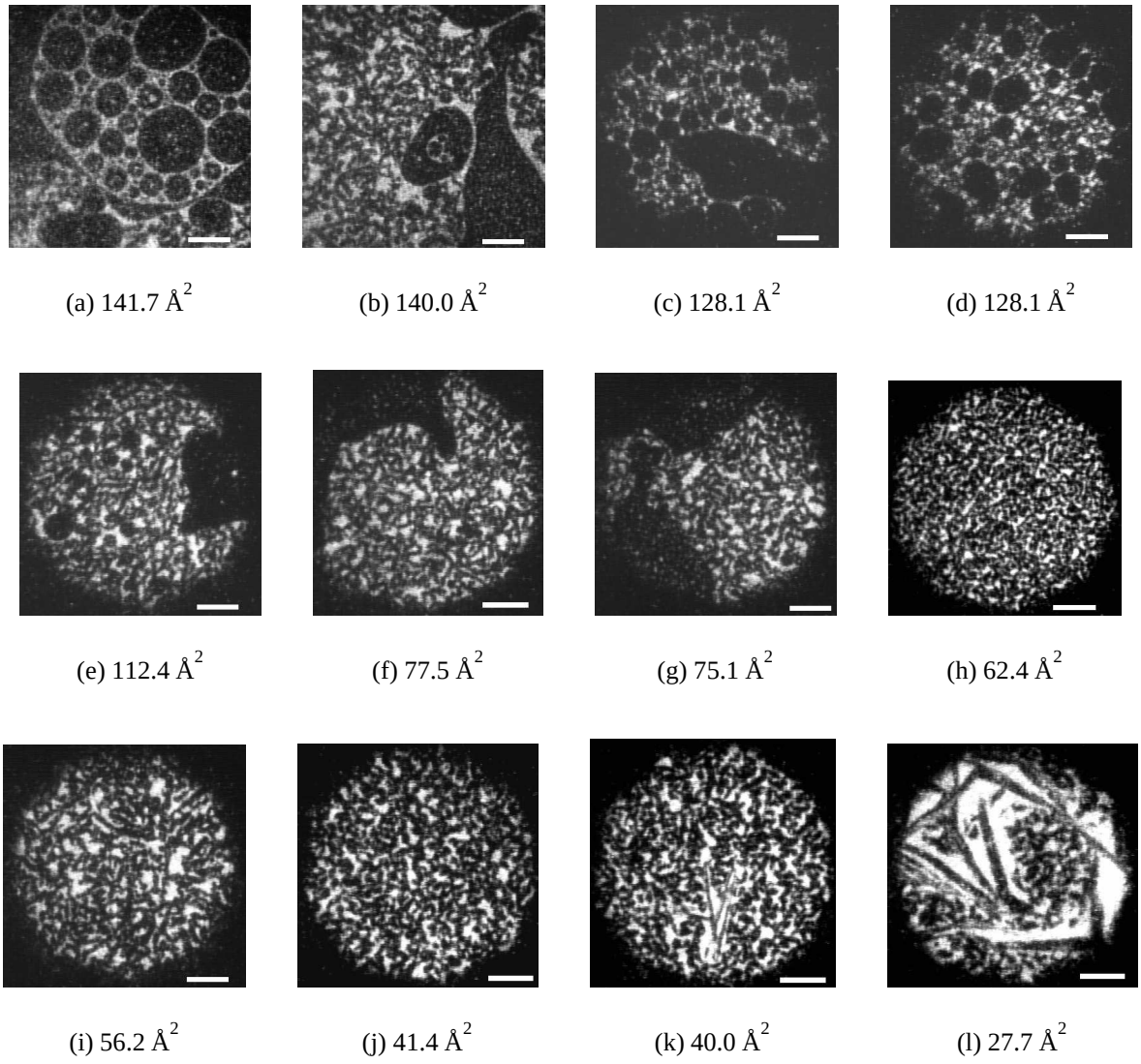

(a) 141.7 Å^2 (b) 140.0 Å^2 (c) 128.1 Å^2 (d) 128.1 Å^2

(e) 112.4 Å^2 (f) 77.5 Å^2 (g) 75.1 Å^2 (h) 62.4 Å^2

(i) 56.2 Å^2 (j) 41.4 Å^2 (k) 40.0 Å^2 (l) 27.7 Å^2

Figure 4.7: Epifluorescence images for cholesteryl acetate. Figures (a) to (g) show the co-existing gas(dark) + L_2 domains. With decreasing A/M, the circular G domains diminish in size. The L_2 phase appears as a bright mesh network with irregular boundaries. Figures (h) to (j) show the predominantly present L_2 phase. Figures (k) and (l) show the collapsed state. Here, long needle like crystals appear from the background L_2 phase. Scale bar represents 50 μm.

epifluorescence images for 0.5 MF of ChA are shown in Figure 4.9. Above 45Å^2, the co-existence of gas + L_1 phase is observed. Upon compression, the L_1 phase grows at the expense of gas phase. Above the lower collapse pressure($\pi_{c(8CB)}$), the nucleation of 8CB multilayers(D_2) were seen to increase in number(Figures 4.9(a) to 4.9(c)). Above the second collapse pressure($\pi_{c(ChA)}$), ChA crystallites were seen to coexist with D_2 domains. This is

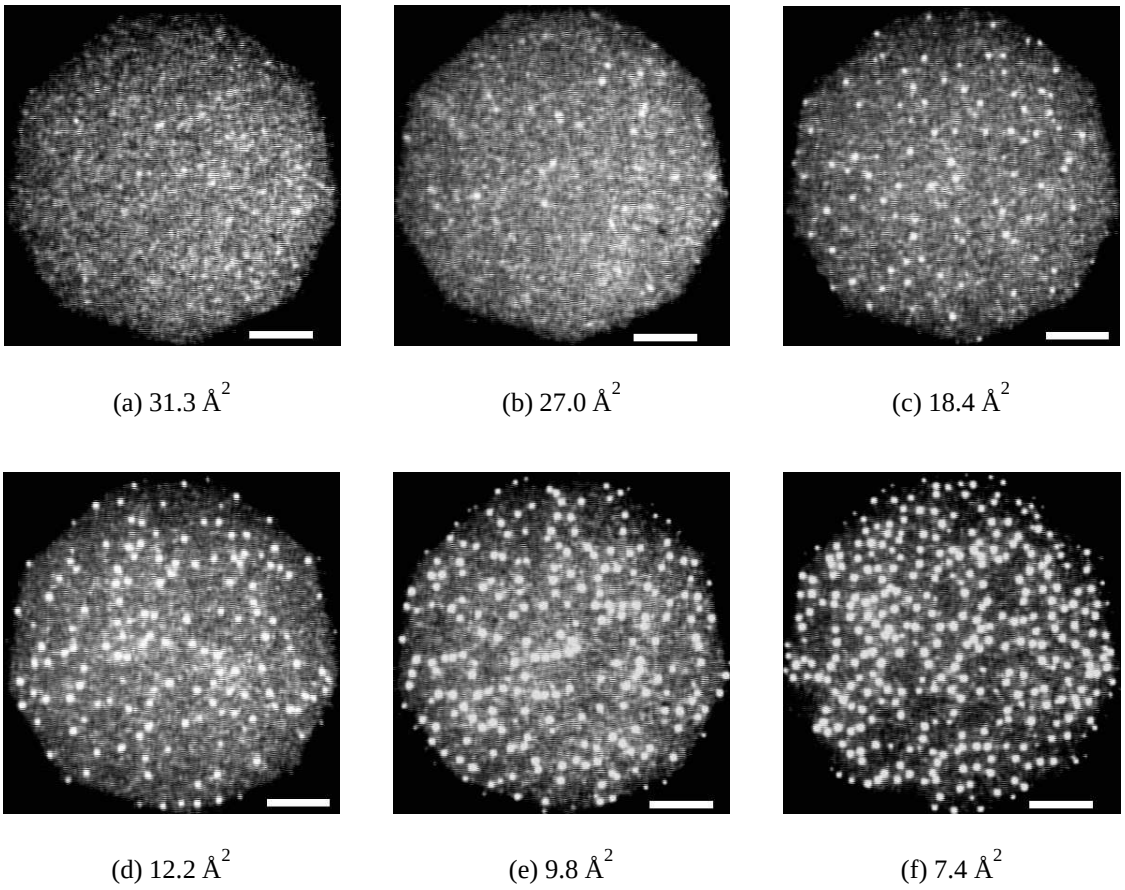

(a) 31.3 Å^2 (b) 27.0 Å^2 (c) 18.4 Å^2

(d) 12.2 Å^2 (e) 9.8 Å^2 (f) 7.4 Å^2

Figure 4.8: Epifluorescence images at 0.25 MF of ChA in ChA-8CB mixed films at the A-W interface. Figures (a) to (f) show the collapsed state. Figures (a) to (d) show small bright spots which are multilayers(D_2) coexisting with L_1 phase(above $\pi_{c(8CB)}$). Figures (e) and (f) show the brighter multilayer D_2 domains with the ChA crystals in the background(above $\pi_{c(ChA)}$). Scale bar represents 50 μm.

shown in Figures 4.9(d) to 4.9(g). The epifluorescence images for 0.75 MF of ChA in 8CB is shown in Figure 4.10. The mixed monolayer at this MF of ChA shows the coexisting gas + L_1 phase(Figures 4.10(a) and 4.10(b)). Above the lower collapse pressure, $\pi_{c(8CB)}$, very few bright spots were seen which were D_2 phase. Above the second collapse pressure, $\pi_{(ChA)}$, the ChA crystallites nucleate and grow(Figures 4.10(d) to 4.10(h)).

Brewster angle microscopy was used to analyze the collapsed states of the mixed monolayer of ChA-8CB system. This is shown in Figure 4.11. The collapsed state of the mixed monolayer above $\pi_{c(8CB)}$ is shown in Figure 4.11(a). The appearance of small bright spots are the indication of the formation of 8CB multilayers. Above $\pi_{c(ChA)}$, long bright needle

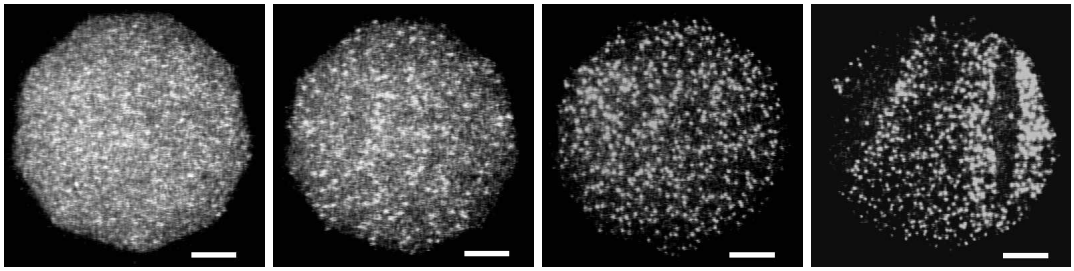

(a) 26.1 Å^2 (b) 23.7 Å^2 (c) 19.0 Å^2 (d) 13.5 Å^2

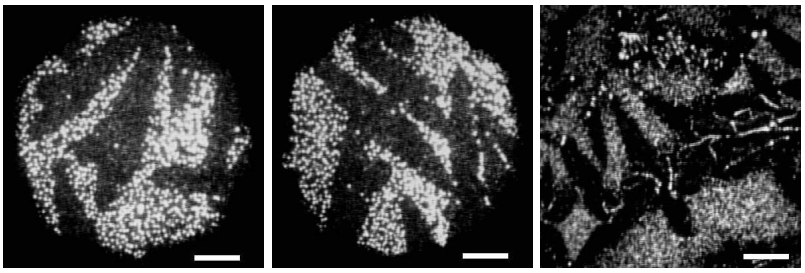

(e) 10.7 Å^2 (f) 8.7 Å^2 (g) 7.6 Å^2

Figure 4.9: Epifluorescence images at 0.5 MF of ChA in ChA-8CB mixed films at the A-W interface. Figures (a) to (c) represent the $L_1 + D_2$ phase coexistence. Here the small but bright D_2 domains coexist with the background L_1 phase. Figures (d) to (g) show ChA crystallites coexisting with D_2 domains. The ChA crystallites appeared dark in contrast coexisting with the much brighter D_2 domains in the background. Scale bar represents 50 μm.

shaped crystallites were seen to coexist with the 8CB multilayers(Figure 4.11(b)). The variation of collapse pressure and the observation of the phases indicated miscibility below the lower collapse pressure($\pi_{c(8CB)}$). To analyse the stability and the condensation in the mixed monolayer the deviation from the ideal area, the excess area and the excess Gibbs Free energy were calculated. The plot of ideal A/M, A_{id} and the experimentally determined A/M, A_{12} with increasing MF of ChA in 8CB are shown in Figure 4.12. There was a considerable deviation of the A_{12} from the ideal case. The excess area(A_{exc}) can be determined from the difference between the experimentally determined A/M(A_{12}) and the ideal A/M(A_{id}). i.e., ($A_{exc} = A_{12} - A_1X_1 - A_2X_2$). The excess Gibbs free energy was calculated from the isotherm for the mixed monolayer of ChA-8CB system. The excess Gibbs free energy, ΔG_{exc}, for the mixed monolayers at constant surface pressures were obtained by integrating the excess area

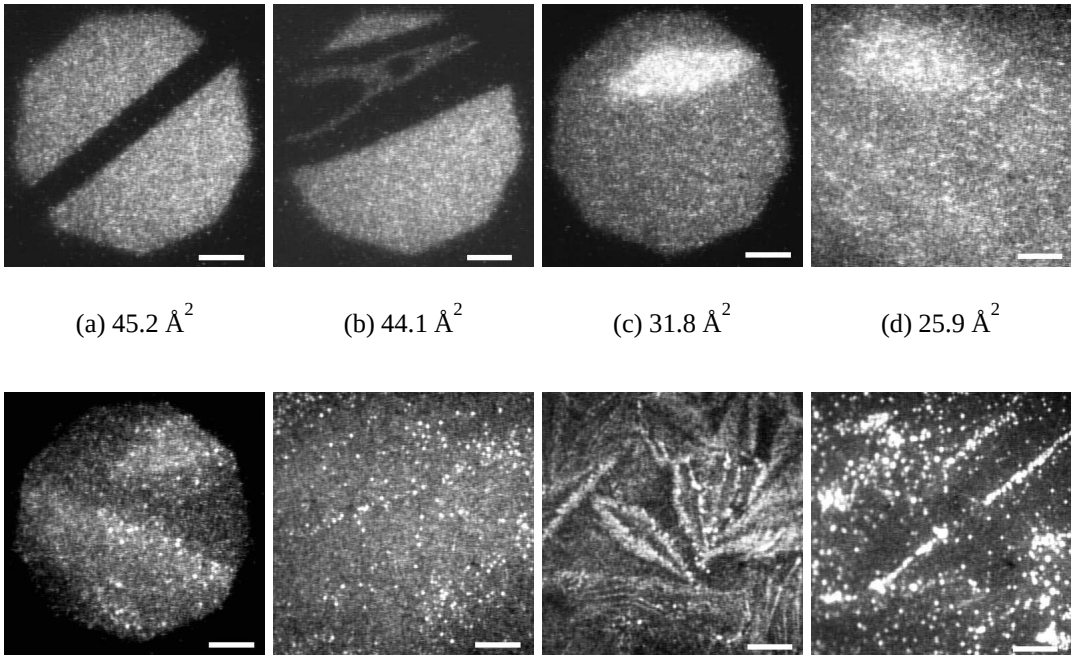

(a) 45.2 Å^2 (b) 44.1 Å^2 (c) 31.8 Å^2 (d) 25.9 Å^2

(e) 21.4 Å^2 (f) 19.4 AA^2 (g) 10.3 Å^2 (h) 7.8 Å^2

Figure 4.10: Epifluorescence images at 0.75 MF of ChA in ChA-8CB mixed monolayers at the A-W interface. Figures (a) and (b) represent the coexisting gas(dark) + L_1 phase. Figures (c) to (h) show the collapsed state. Here, the small bright spots are the multilayers(D_2) and the elongated structures are the 3D crystals of ChA. Scale bar represents 50 μm.

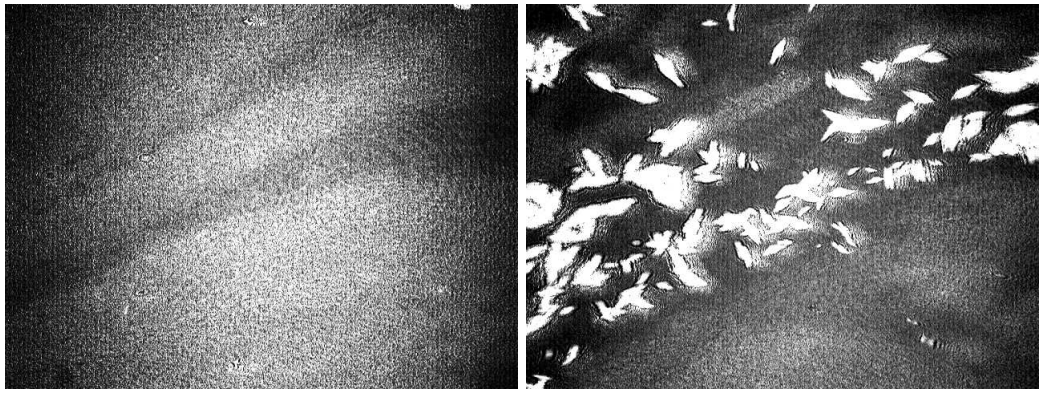

(a) 26.1 Å^2 (b) 19.9 Å^2

Figure 4.11: Brewster angle microscopy images at 0.5 MF of ChA in 8CB. Figure(a) represents the collapsed state(above $\pi_{c(8cb)}$). Here, the small bright spots are the multilayers(D_2) which coexist with the L_1 phase(background). Figure(b) represents the collapsed state(above $\pi_{c(ChA)}$). Here, the very bright needles are 3D crystals of ChA which coexist with small bright spots which are the multilayer(D_2) domains. Scale of each image is 6.4 x 4.8 mm^2.

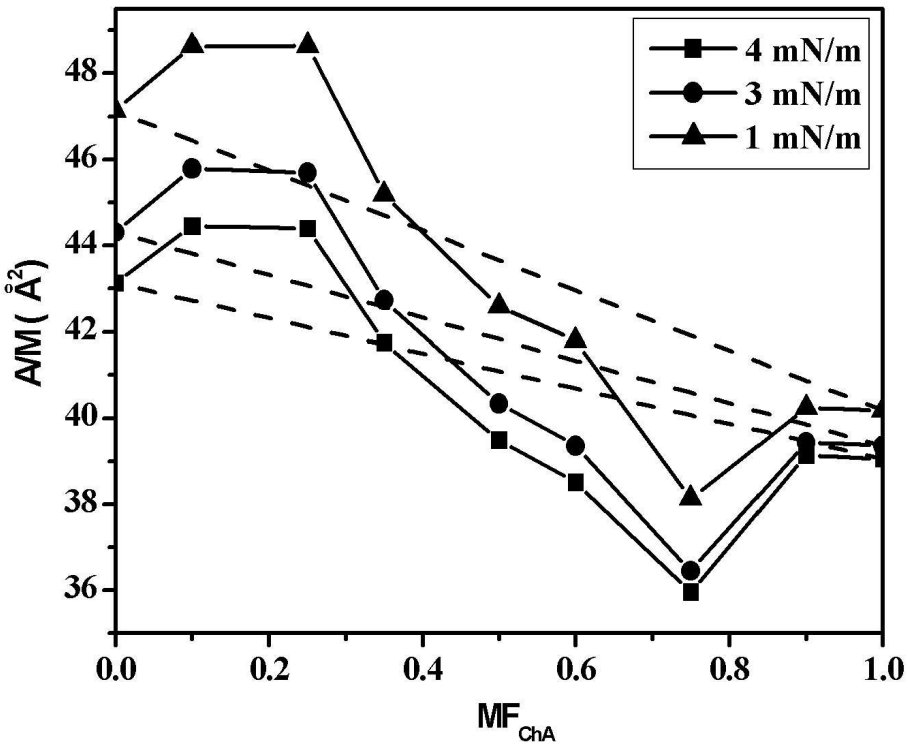

Figure 4.12: The variation of the experimentally determined area per molecule, A_{12}, continuous lines and the calculated ideal area per molecule, A_{id}, dashed lines with MF of ChA in ChA-8CB mixed monolayers at different surface pressures. The difference between A_{12} and A_{id} will give the excess area A_{exc} .

over surface pressure [7]. It is given by,

$$\Delta G_{exc} = N_a \int_{\pi^*}^{\pi} (A_{exc}) d\pi \tag{4.2}$$

Here, π^* is the surface pressure at which the two components of the mixed monolayer behave ideally(which is usually taken as zero) and N_a is the Avogadro number. A negative value of the excess Gibbs free energy for the mixed monolayer indicates that the interactions are attractive. On the other hand, if it is positive then the interactions are of repulsive nature. The excess Gibbs free energy is plotted against the MF of ChA(Figure 4.13). This was calculated for different surface pressures below the 8CB collapse pressure(4.7 mN/m). The mixed monolayer exhibits a positive maximum at 0.35 MF and negative at higher compositions of ChA. Based on the surface manometry, epifluorescence, BAM studies and the

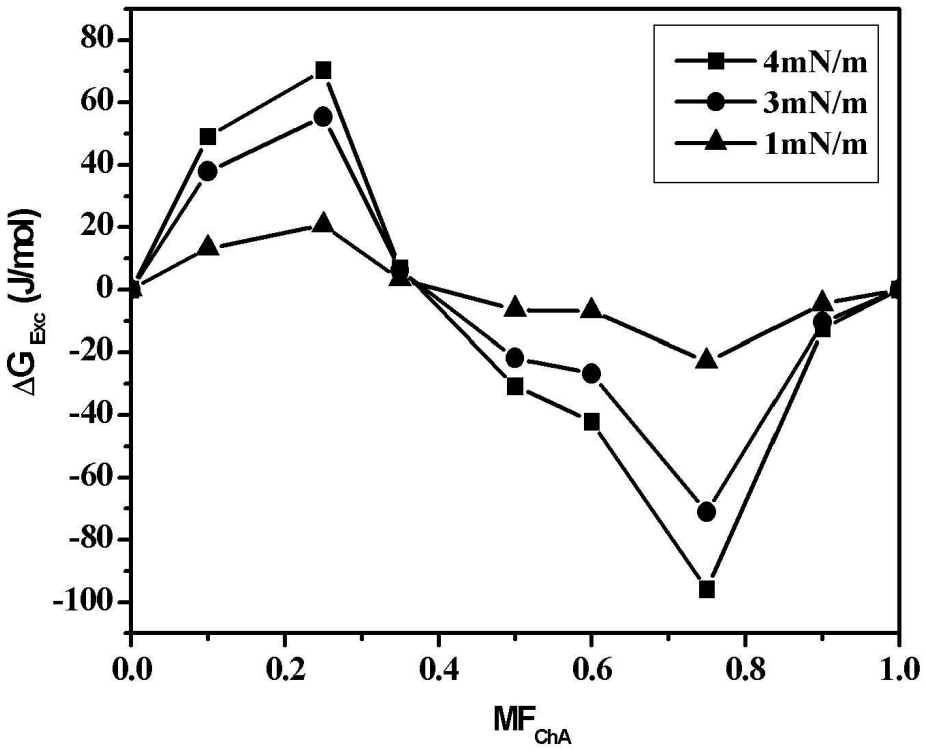

Figure 4.13: Variation of excess Gibbs free energy, ΔG_{exc} with mole fraction(MF) of ChA in 8CB, computed at different surface pressures.

thermodynamic analysis we have constructed a phase diagram for the mixed monolayer of ChA-8CB system. This is shown in shown in Figure 4.14.

4.4 Discussions

The mixed monolayer behavior of ChA-8CB was investigated using surface manometry, epi-fluorescence, BAM studies and thermodynamic analysis. The individual monolayer behavior of ChA suggests that the relatively less polar ester group tends to form a stable monolayer The limiting area per molecule, A_0, for Ch and ChA obtained by extrapolating the area at collapse were comparable. This indicated that ChA molecules were nearly normal to the A-W interface.

We find from epifluorescence microscope studies that ChA monolayer exhibits bright

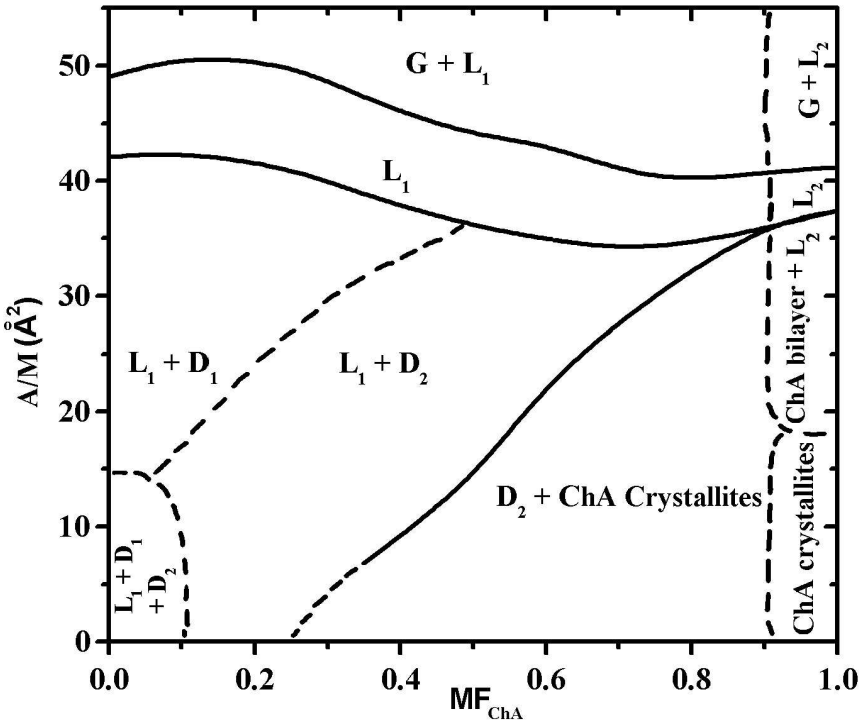

Figure 4.14: Phase diagram for ChA - 8CB mixed monolayer at t=22 °C. Here, the continuous lines indicate the actual phase boundaries and the dashed lines indicate the approximate phase boundaries.

meshy textures in L_2 phase which is crystalline in nature. This is in agreement with the grazing incidence X-ray diffraction(GIXD) experiments on the monolayer of ChA indicated enhanced crystallinity at very large A/M [8]. They have reported that ChA possess pseudo rectangular lattice with the lattice parameters, a=10.14 Å, b=7.48 Å and γ=92.2 °. Further, the monolayer phase of ChA was more crystalline than the monolayer of Ch. The presence of weakly polar ester group in ChA tends to make the monolayer more crystalline in nature.

The trend in the collapse pressure behavior for ChA-8CB mixed monolayer was different from that of Ch-8CB mixed monolayer. The variation of lower collapse pressure($\pi_{c(8cb)}$) with increasing composition of ChA in 8CB indicated that the monolayer is miscible below this collapse pressure. This shows that the presence of ChA in 8CB enhances the stability of the mixed monolayer. We observed the phase separation occurring above lower collapse pressure by spontaneous nucleation of the multilayers(D_2). After higher collapse region,

these D_2 domains were seen to coexist with collapsed crystallites of ChA. We attribute this observed miscibility below the lower collapse pressure to the dipole induced dipole interaction between the C≡N group of 8CB and -OCO group of ChA. Similar trend in the collapse pressure behavior was observed for the mixed monolayer of Ch with unsaturated fatty acids [6]. Here also the lower collapse pressure increased with composition and the higher collapse pressure was independent of composition. Here, the degree of saturation was varied by increasing the double bond in the alkyl chains.

The tendency to form hydrogen bonding network with water is less for ChA(only hydrogen bond acceptor) when compared to OH in Ch(both hydrogen bond donor and acceptor). The degree of hydration or solvation for OCO polar group in ChA is less when compared with OH polar group of Ch. Thus the ester group in ChA has the tendency to bind with low affinity with water molecules at the interface. The orientation of bounded water molecules surrounding the CN dipole can exist as in the previous case for Ch-8CB system. The presence of weakly polar ester in ChA interacts with the CN dipole of 8CB resulting in miscibility below the lower collapse pressure($\pi_{c(8CB)}$). The bridging water molecules might also have a role to play. However, above the lower collapse pressure($\pi_{c(8CB)}$), the monolayer phase separates.

For ChA-8CB mixed monolayer, below the lower collapse pressure, $\pi_{c(8CB)}$, the monolayer is miscible. The miscibility nature of ChA-8CB mixed monolayer can be explained using Crisp's phase rule [9]. Applying equation(3.1) of chapter-3 to ChA - 8CB mixed monolayer, if C_b=2(air and water), C_s=2(ChA and 8CB) and P_b=3(gas, liquid and D_1), then, F=2-q. If there is only one monolayer phase(q=1) then, F=1. This implies that the collapse pressure should vary with the composition of the mixed monolayer in agreement with the results.

The miscibility studies on weakly polar ester group of ChA and strongly polar CN group of 8CB was investigated. The mixed monolayer exhibit L_1 phase nearly at all composition which and was uniform in appearance under epifluorescence. Unlike the case of Ch and 8CB, we did not observe any phase separation in the mixed monolayer of ChA and 8CB below the lower collapse pressure. The polar OH group in Ch is shielded effectively by the

water molecules because of its donor and acceptor hydrogen bonding ability. The strongly polar CN group in 8CB which acts as hydrogen bond acceptor polarizes the environment and reorient the water molecules and thus changes locally the hydrogen bonded network. This mismatch in the orientational differences between the water molecules might be the probable the reason for the observed immiscibility in the case of Ch-8CB mixed monolayer. However, in ChA, the weakly polar OCO group acts only as an hydrogen bond acceptor with relatively less hydrogen bonding formation with water molecules. The OCO group of ChA can also interact with the CN group of 8CB through dipole-induced dipole interactions favoring the miscibility and immiscible above lower collapse pressure due to weaker interactions between the hydrophobic parts.

Bibliography

[1] W.J. Foster, M.C. Shih and P.S. Pershan, J. Chem. Phys., **105**, 3307, 1996.

[2] G.L. Gaines Jr., *Insoluble monolayers at air-water interface,* Wiley-Interscience, 1966.

[3] K.S. Birdi, *Lipid and biopolymer monolayers at liquid interfaces*, Plenum:NY, 1989. 677, 2000.

[4] G.R. Desiraju and T. Steiner, *The weak hydrogen bond : In structural chemistry and biology*, Oxford Science Publications, 1999.

[5] X. Li, M.M Momsen, J.M. Smaby, H.L. Brockman and R.E. Brown, Biochem. **40**, 5954, 2001.

[6] R. Seoane, P. Dynarowicz-tstka, J. Minones Jr and I. Rey-Gomez-Serranillos, Coll. Poly. Sci., **279**, 562, 2001.

[7] F.C. Goodrich, *Proc. 2nd International Congress on Surface Activity*, Butterworth, London, vol. I, M33, 1957.

[8] H. Rapaport, I. Kuzmenko, S. Lafont, K. Kjaer, P.B. Howes, J. Als-Nielsen, M. Lahav and L. Leiserowitz, Biophys. Jour., **81**, 2729, 2001.

[9] D.J. Crisp, *Surface Chemistry Suppl. Research*, Butterworths:London, 1949.